2002 2

2002 2

<u>୧</u>)

<u>인</u>

ହା

ABSTRACT	
·	2
	4
- 1.	4
- 2.	7
- 2- 1.	7
- 2- 2.	12
- 2- 3.	22
•	27
- 1.	27
- 2.	30
	42

A Study for Characteristics Analysis and Radiation Characteristics Improvement of

Parametric Transmitter in Air.

## Byung-Cheon Moon

Interdisciplinary Program of Acoustics and Vibration Engineering, Graduate School.

Pukyong National University

## **ABSTRACT**

Recently, a sound source with high directivity has being studied for audio industry.

Parametric array performed by nonlinear effect of sound wave can make a sound source with high directivity. However, the sound source in air, generally, use a flexural type vibrator with the large amplitude in low frequency range. In such kinds of vibrators, it is difficult to analyze their characteristics on the assuming that the sound pressure distribution of vibrating surface is piston sound source. And its vibration center has 180, out of phase with its edge in resonance modes so that the side-lobe levels are high.

In this paper, to be applied a parametric method to a sound transmitter, the directional sound source is made by arrayed devices to generate ultrasonic in air and with low resonance frequency relatively. Behaviors of primary wave radiating from the parametric transmitter and secondary wave generating in a propagating process are investigated. From the result of experiment, a possibility for development and directivity characteristics improvement of parametric transmitter in air is investigated.

, 가

,

, 가

가

가 . 가 ,

, 가

Westervelt [1-6].

가

[7].

[8- 11]. , 가

.

type vibrator )7} . , ,

가 180° 가 ,

가 가

가

가

가

- 3 -

•

- 1.

Westervelt a

, Lighthill z , heta

 $p_d$  (1)

$$p_{d} = -\frac{j \beta k_{d}^{2} a^{2} p_{01} p_{02}}{4 \alpha_{T} \rho_{0} c_{0}^{2}} \frac{\exp(-\alpha_{d} z)}{z} D_{W}(\theta) D_{A}(\theta)$$

$$D_{W}(\theta) = \frac{1}{1 + j 2 (k_{d} / \alpha_{T}) \sin^{2}(\theta / 2)}$$

$$D_{A}(\theta) = \frac{2 J_{1} (k_{d} a \sin \theta)}{k_{d} a \sin \theta}$$
(1)

$$, \beta = 1 + \frac{B}{2A},$$

$$k_d = \frac{(\omega_1 - \omega_2)}{c_0},$$

 $p_{01}, p_{02}$  2

$$\alpha_T = \alpha_1 + \alpha_2 - \alpha_d,$$

 $\alpha_1, \quad \alpha_2$ 

 ${\cal C}_d$  .

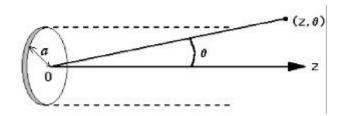


Fig. 1.

Fig. 1 Parametric array for circular piston source

Fig. 1 Westervelt

, , 
$$Tj\phi$$
tta

7\ [12-13].  $a$ 
 $p_{0i}(r)$  ,  $(r,z)$ 

 $p_i, p_d$  .

$$p_{i}(r,z) = -j\frac{k_{i}}{z} \exp\left(-\alpha_{i}z + \frac{jk_{i}r^{2}}{2z}\right) \times \int_{0}^{a} \exp\left(\frac{jk_{i}r^{2}}{2z}\right) p_{0i}(r') J_{0}\left(\frac{r'r}{z}\right) r' dr'$$
(2)

$$p_{d}(r,z) = -j \frac{\beta k_{1} k_{2} k_{d}}{2 \pi \rho_{0} c_{0}^{2} z} \exp \left(-\alpha_{d} z + \frac{j k_{d} r^{2}}{2 z}\right)$$

$$\times \int_{z'=0}^{z} \int_{\phi=0}^{\pi} \int_{r_{1}=0}^{a} \int_{r_{2}=0}^{a} \exp \left(j \frac{k_{1} r_{1}^{2} - k_{2} r_{2}^{2}}{2 z}\right)$$

$$\times \exp \left[-\alpha_{T} z' + j G\left(\frac{1}{z} - \frac{1}{z'}\right)\right] J_{0}\left(\frac{r}{z} \sqrt{F}\right)$$

$$\times p_{01}(r_{1}) p_{02}(r_{2}) \frac{r_{1} r_{2}}{z'} dr_{2} dr_{1} d\phi dz'$$
(3)

, 
$$F = k_1^2 r_1^2 + k_2^2 r_2^2 - 2k_1 r_1 k_2 r_2 \cos \phi$$
,  
 $G = k_1 k_2 (r_1^2 + r_2^2 - 2r_1 r_2 \cos \phi) / (2k_d)$ 

$$p_{d}(r,z) = -j \frac{\beta k_{1} k_{2} k_{d}}{2\pi \rho_{0} c_{0}^{2} z} \exp\left(\frac{j k_{d} r^{2}}{2 z}\right)$$

$$\times \int_{\phi=0}^{\pi} \int_{r_{1}=0}^{a} \int_{r_{2}=0}^{a} \exp\left(\frac{j G}{z} + j \frac{k_{1} r_{1}^{2} - k_{2} r_{2}^{2}}{2 z}\right)$$

$$\times E_{1} \left(j \frac{G}{z}\right) J_{0} \left(\frac{r}{z} \sqrt{F}\right) p_{01}(r_{1}) p_{02}(r_{2}) r_{1} r_{2} dr_{2} dr_{1} d\phi$$

$$, E_{1}(x) \qquad \int_{r}^{\infty} \frac{\exp(-t)}{t} dt \qquad .$$
(4)

 $\int_{x}^{\infty} \frac{\exp(-t)}{t} dt$ 

 $p_{0i}(r)$  Bessel Gauss

가 가 ,

가 .

, 가 가

,

가 가 .

 $(2) \qquad (4)$ 

- 2. - 2- 1.

Fig. 2
. 4.5mm PZT 5.9mm
, Network Analyzer
42.75kHz , Fig. 3 .

1kHz 42.25kHz 43.25kHz

Fig. 4

GRAPHTEC AT 3500 Laser Vibrometer

,

Bessel

Fig. 5 .

Fig. 5 3mm 가 (-)

180° . , (+)

,

가 .

가 .

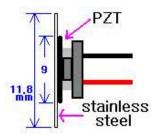






Fig. 2

Fig. 2 Shape of flexural type vibrator

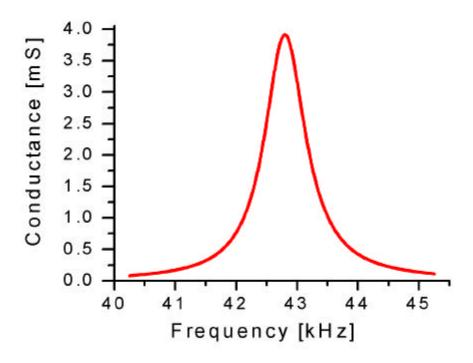


Fig. 3
Fig. 3 Result of frequency response measurement

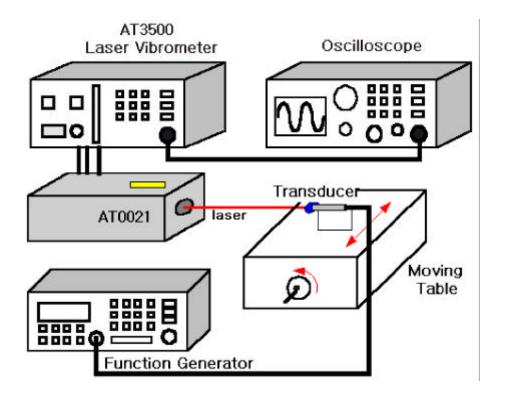


Fig. 4
Fig. 4 Block diagram of experimental setup
for vibration distribution measurement

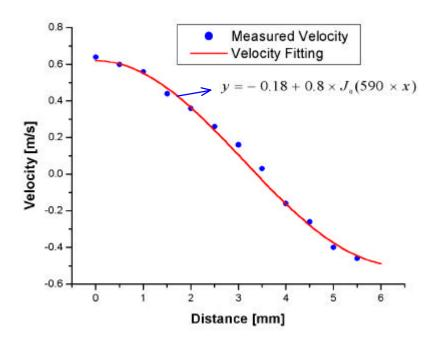


Fig. 5
Fig. 5 Measured result of vibration distribution and fitted curve

-2-2.

(2) (4)

Bessel

Fig. 6 Fig. 7

Bessel

, Bessel 45 °

, Bessel 가 Fig. 8

, Fig. 9 .

Fig. 9 ,

· , 가

, Bessel Gauss

Fig. 10 Fig. 13 .

Fig. 11 Bessel

, 가 가 가 .

, Fig. 13 Gauss

.

가 . ,

가 가 .

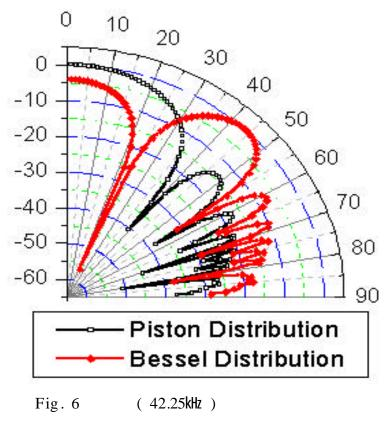


Fig. 6 Comparison to directivity pattern of primary wave (42.25kHz)

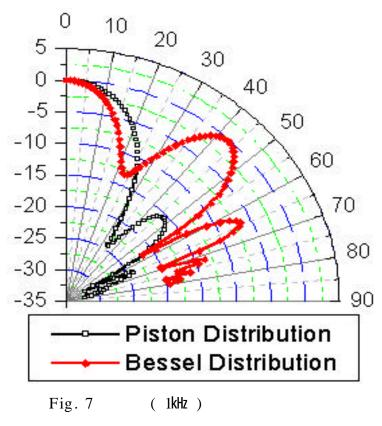


Fig. 7 Comparison to directivity pattern of secondary wave (1kHz)

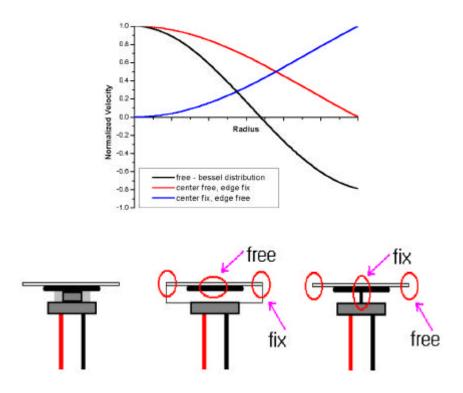
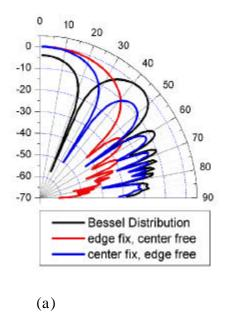


Fig. 8

Fig. 8 Change of vibration distribution pattern

by boundary condition of vibrator



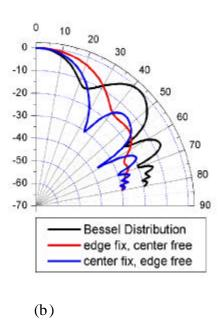


Fig. 9

Fig. 9 Simulation results of parametric array for vibration distribution pattern

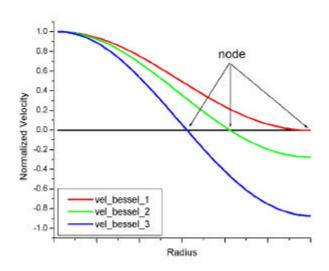


Fig. 10 Bessel

Fig. 10 Change of vibration distribution pattern by node of Bessel distribution type vibrating mode

node

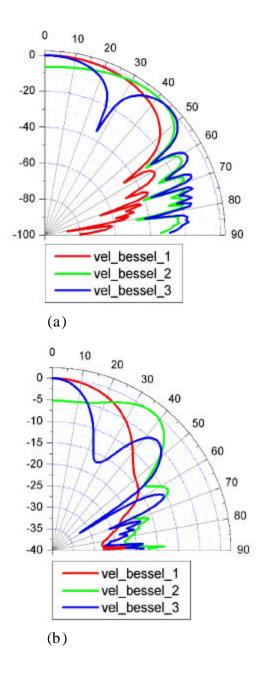


Fig. 11 Bessel node

Fig. 11 Simulation results of parametric array for various with nodes of Bessel type vibrating distribution

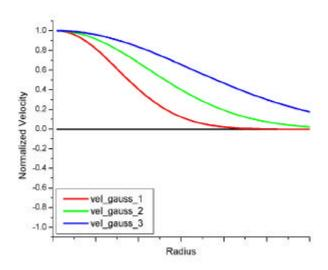


Fig. 12 Gauss

Fig. 12 Change of vibration distribution pattern by covariance of Gauss type vibrating mode

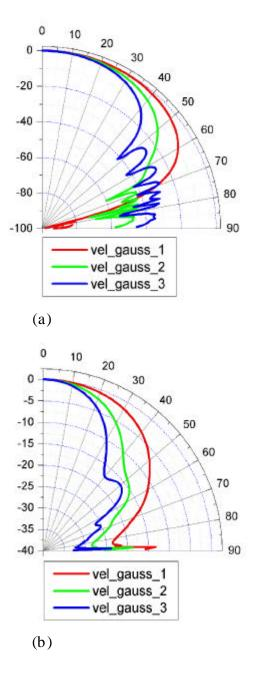


Fig. 13 Gauss

Fig. 13 Simulation results of parametric array for various covariance of Gauss type vibrating distribution

- 2- 3.

가 Fig. 14 Function Generator ( HP8904A ) 42.25kHz 43.25kHz  $6V_{pp}$ 가 60V<sub>pp</sub> 10 가 , Condenser type Microphone (B&K Type 4135) 가 FFT Analyzer Digital Oscilloscope 100mm 0 ° 80° 1° Fig. 15 Primary 42.25kHz , Difference 1kHz Fig. 15 45dB re  $20\mu$ Pa 가 55° 가 Bessel Bessel 가 Fig. 16 Fig. 17 가 Fig. 16 Bessel 50° Fig. 17 Fig. 16 가 50°

가

•

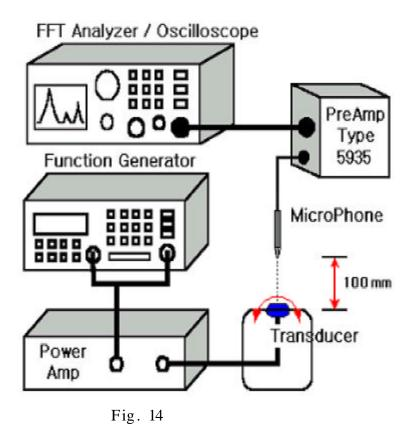


Fig. 14 Experimental setup for directivity measurement

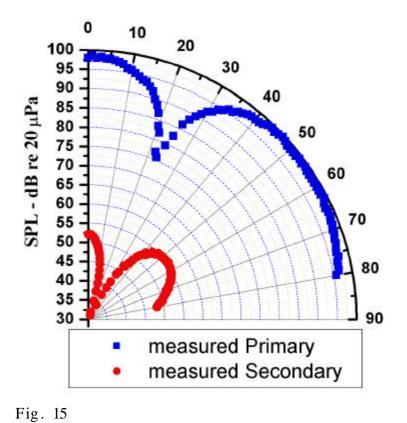


Fig. 15 Result of directivity characteristics measurement of parametric array

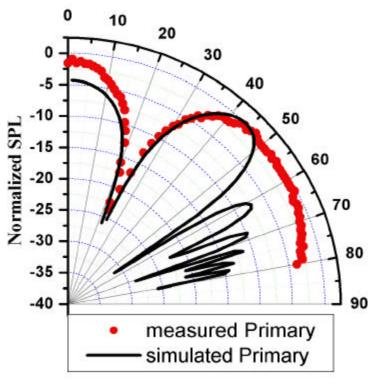


Fig. 16

Fig. 16 Comparison of directivity pattern of primary wave

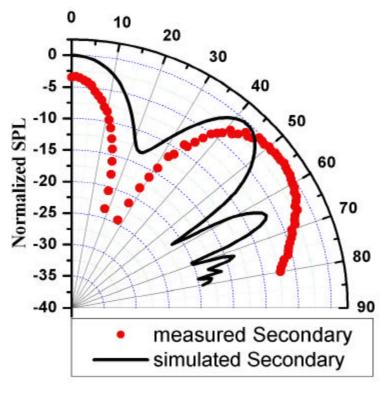


Fig. 17

Fig. 17 Comparison of directivity pattern of secondary wave

- 1.

50° .

50 °

Fig. 19 
$$\phi$$

Tj $\phi$ tta (2) (4) . . , 90 ° . . . 7

, 가 . 가

source strength  $m\,Q$  , source strength Q

, 180 ° Fig. 18 . (5)

$$H(\theta) = \frac{m}{m-2} - \frac{2}{m-2} \cos\left(\frac{kd}{2}\sin\theta\right)$$
 (5)

가 Fig. 19

Product theorem [14] (6)

.

$$H(\theta) = \left[\frac{m}{m-2} - \frac{2}{m-2} \cos\left(\frac{kd}{2}\sin(\theta + \phi)\right)\right] \times \left[\frac{m}{m-2} - \frac{2}{m-2}\cos\left(\frac{kd}{2}\sin(\theta - \phi)\right)\right] \times \cos\left(\frac{kl}{2}\sin\theta\right)$$
(6)

(6)

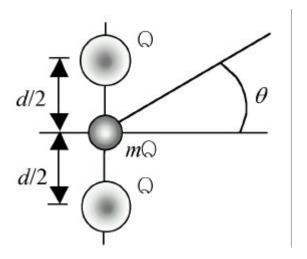


Fig. 18

Fig. 18 Simulation model for single flexural type vibrator

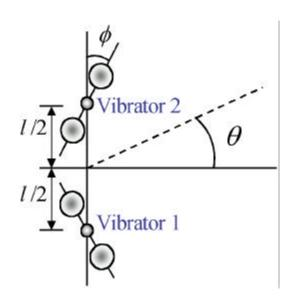


Fig. 19

Fig. 19 Simulation model for arrayed flexural type vibrator

- 2.

Fig. 20 PZT 3**mm** 4.5 mm2 Network Analyzer 44.38 kHz45.47kHz Laser Vibrometer (GRAPHTEC AT 3500) , Fig. 21 . Fig. 21 (-) . Fig. 21 (+)Fig. 18 가 가 l $\phi$ l가  $\phi$ (6) l 가  $18 \mathrm{mm}$ 20 mm $\phi$  $18 \mathrm{mm}$ l50°, *l* 20mm 62° Fig. 22 Fig. 23 Fig. 24

Function Generator 10V<sub>pp</sub>

 $V_{pp}$  가 ,

Power Amp  $60V_{\mathfrak{p}\mathfrak{p}}$ , Condenser type Microphone ( B&K Type 4135 ) 120mm FFT Analyzer Digital Oscilloscope 가 45.29kHz 46.29kHz 가 1kHz 가 (6) Fig. 25 Fig. 26 . Fig. 25 (a) 가 0.9 , 50° 1.25 (b) 2.86 Fig. 26 (a) 0.9 (b) 1.54 50° 2 Fig. 25 Fig. 26 Fig. 25(a), Fig. 26(a)  $\phi$ Fig. 25(b), Fig. 26(b) Fig. 27 Fig. 28 Fig. 27 , (a)

- 32 -

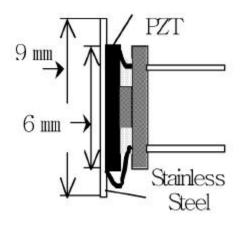




Fig. 20
Fig. 20 Shape of flexural type vibrator used in experiment

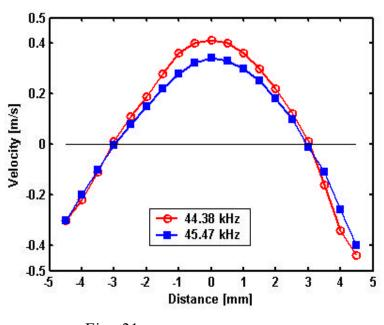
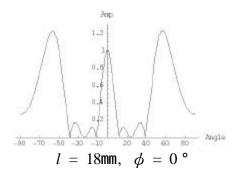
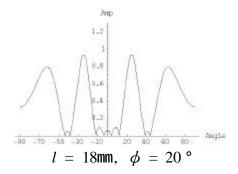
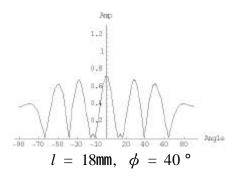


Fig. 21

Fig. 21 Measurement results of vibration distribution







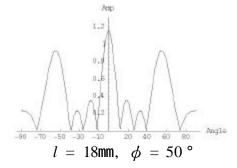
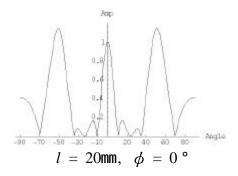
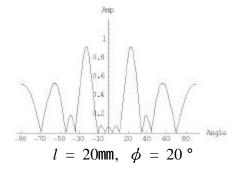
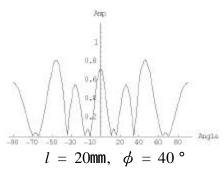


Fig. 22 l = 18mm  $\phi$ 

Fig. 22 Simulation results of primary wave for various  $\phi$  at l=18mm







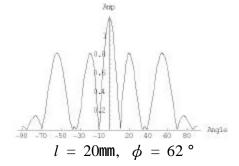


Fig. 23 l = 20mm  $\phi$ 

Fig. 23 Simulation results of primary wave for various  $\phi$  at l=20mm

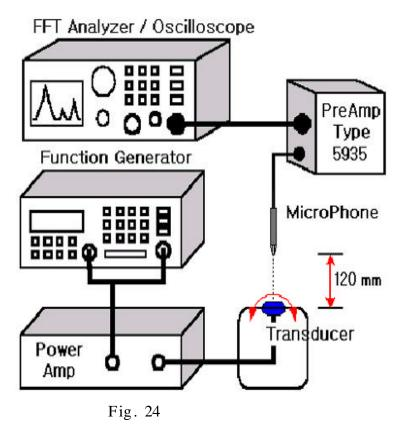
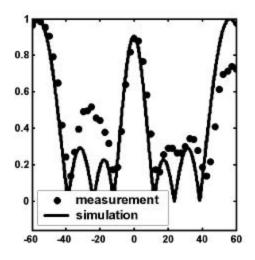
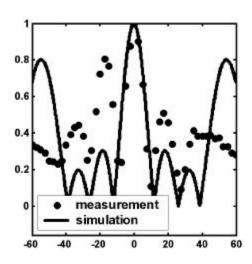


Fig. 24 Experimental setup for directivity measurement

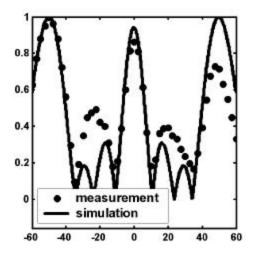


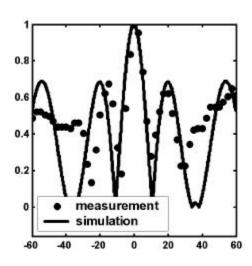


(b)  $\phi = 50^{\circ}$ 

Fig. 25 l = 18mm

Fig. 25 Change of directivity characteristics for  $\phi = 0$  ° and  $\phi = 50$  ° at l = 18mm

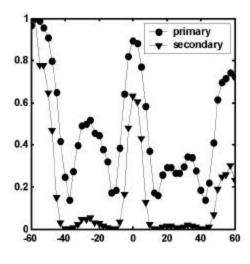


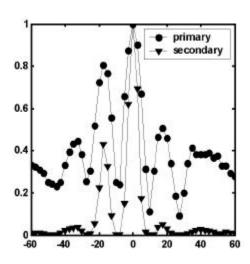


(b)  $\phi = 62^{\circ}$ 

Fig. 26 l = 20 mm

Fig. 26 Change of directivity characteristics for  $\phi = 0$  ° and  $\phi = 62$  ° at l = 20mm

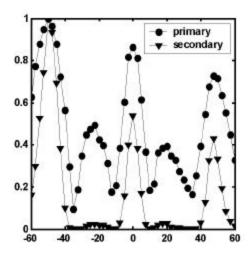


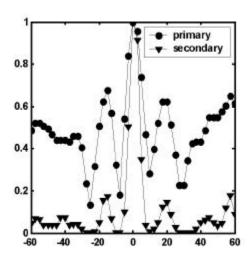


(b)  $\phi = 50^{\circ}$ 

Fig. 27 l = 18mm

Fig. 27 Change of directivity characteristics for  $\phi = 0$  ° and  $\phi = 50$  ° at l = 18mm





(b)  $\phi = 62^{\circ}$ 

Fig. 28 l = 20 mm

Fig. 28 Change of directivity characteristics for  $\phi = 0$  ° and  $\phi = 62$  ° at l = 20mm

Bessel 가

50°

가

가 가

가

, 50° *l* 18mm 1.25 2.86

, *l* 20mm 1.54

- 42 -

50° 2

가 *l* 18mm 2.5 , 50°

20

, l 20mm 5.6

, 50° 10

,

가 .

- [1] P. J. Westervelt: "Parametric Acoustic Array", J. Acoust. Soc. Am, 35(4), pp. 535-537, 1963.
- [2] T. G. Muir and J. G. Willette: "Parametric Acoustic Transmitting Arrays", J. Acoust. Soc. Am., 52(5), pp. 1481-1486, 1972.
- [3] M. B. Moffett, P. J. Westervelt and R. T. Beyer: "Large Amplitude Pulse Propagation-A Transient Effect", J. Acoust. Soc. Am., 47(5), pp. 1473-1447, 1970.
- [4] Richard L. Rolleigh: "Difference Frequency Pressure within the Interaction Region of a Prarmetric Array", J. Acoust. Soc. Am., 58(5), pp. 964-971, 1975.
- [5] H. O. Berktay and D. J. Leahy: "Farfield Performance of Parametric Transmitters", J. Acoust. Soc. Am., 55(3), pp. 539-546, 1974.
- [6] 鎌 倉 友 男 : "Fundamentals of Nonlinear Acoustics", 愛智出版, 東京, 1996.
- [7] H. O. Berktay: "Possible Exploitation of Nonlinear Acoustics in Underwater Transmitting Applications", J. Sound Vib., 2, pp. 435-461, 1965.
- [8] M. B. Bennett and D. T. Blackstock: "Parametric Array in Air", J. Acoust. Soc. Am., 57(3), pp. 562-568, 1975.
- [9] Masahide Yoneyama, Yukawamo, Jun'ichiroh Fujimoto, Shoichi Sasabe: "Application of Nonlinear Parametric Interaction to Loudspeaker", 電子情報通信學會技術研究報告, EA81-65, pp. 41-48, 1981.
- [10] A. I. Kalachev and D. B. Ostrovskii: "Experimental Study of the Near Field of a Parametric Sound Radiator", Sov. Phys. Acoust., 29(3),

- pp. 241-242, 1983.
- [11] Mark B. Moffett and Robert H. Mellen: "On Parametric Source Aperture Factors", J. Acoust. Soc. Am., 60(3), pp. 581-583, 1976.
- [12] 超音波便覽編輯委員會,"超音波便覽", 丸善株式會社, 5章, 1999.
- [13] J. N. Tj $\phi$ tta and S. Tj $\phi$ tta, "Nonlinear equations of acoustics, with application to parametric arrays", J. Acoust. Soc. Am., 69(6), 1644, 1981.
- [14] Lawrence J. Ziomek: "Fundamentals of Acoustic Field Theory and Space-Time Signal Processing", CRC Press, Chapter 7, 1995.

가

,

,

· 가 2